

High Power Linear Arrays of 1.9 μm Laser Diodes

Dr. Gregory H. Olsen
Dr. Jacobus Vermaak

Sensors Unlimited, Inc.
3490 U.S. Route 1, Building 12
Princeton, NJ 08540

April 2001

Final Report

APPROVED FOR PUBLIC RELEASE; DISTRIBUTION IS UNLIMITED



AIR FORCE RESEARCH LABORATORY
Directed Energy Directorate
3550 Aberdeen Ave SE
AIR FORCE MATERIEL COMMAND
KIRTLAND AIR FORCE BASE, NM 87117-5776

20011221 010

Using Government drawings, specifications, or other data included in this document for any purpose other than Government procurement does not in any way obligate the U.S. Government. The fact that the Government formulated or supplied the drawings, specifications, or other data, does not license the holder or any other person or corporation; or convey any rights or permission to manufacture, use, or sell any patented invention that may relate to them.

This report has been reviewed by the Public Affairs Office and is releasable to the National Technical Information Service (NTIS). At NTIS, it will be available to the general public, including foreign nationals.

If you change your address, wish to be removed from this mailing list, or your organization no longer employs the addressee, please notify AFRL/DELS, 3550 Aberdeen Ave SE, Kirtland AFB, NM 87117-5776.

Do not return copies of this report unless contractual obligations or notice on a specific document requires its return.

This report has been approved for publication.

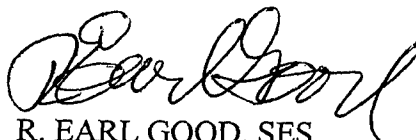


ANDREW ONGSTAD, DR-II
Project Manager



SYLVIA DORATO, DR-III
Chief, Tactical Laser Branch

FOR THE COMMANDER



R. EARL GOOD, SES
Director, Directed Energy

REPORT DOCUMENTATION PAGE				<i>Form Approved</i> OMB No. 0704-0188	
Public reporting burden for this collection of information is estimated to average 1 hour per response, including the time for reviewing instructions, searching existing data sources, gathering and maintaining the data needed, and completing and reviewing this collection of information. Send comments regarding this burden estimate or any other aspect of this collection of information, including suggestions for reducing this burden to Department of Defense, Washington Headquarters Services, Directorate for Information Operations and Reports (0704-0188), 1215 Jefferson Davis Highway, Suite 1204, Arlington, VA 22202-4302. Respondents should be aware that notwithstanding any other provision of law, no person shall be subject to any penalty for failing to comply with a collection of information if it does not display a currently valid OMB control number. PLEASE DO NOT RETURN YOUR FORM TO THE ABOVE ADDRESS.					
1. REPORT DATE (DD-MM-YYYY) 17-04-2001		2. REPORT TYPE Final Report		3. DATES COVERED (From - To) 30/03/1999 - 30/03/2001	
4. TITLE AND SUBTITLE High Power Linear Arrays of 1.9 μ m Laser Diodes				5a. CONTRACT NUMBER F29601-99-C-0030	
				5b. GRANT NUMBER	
				5c. PROGRAM ELEMENT NUMBER 65502F	
6. AUTHOR(S) Dr. Gregory H. Olsen Dr. Jacobus Vermaak				5d. PROJECT NUMBER 3005	
				5e. TASK NUMBER DO	
				5f. WORK UNIT NUMBER AR	
7. PERFORMING ORGANIZATION NAME(S) AND ADDRESS(ES) Sensors Unlimited, Inc. 3490 U.S Route 1, Building 12 Princeton, NJ 08540				8. PERFORMING ORGANIZATION REPORT NUMBER N/A	
9. SPONSORING / MONITORING AGENCY NAME(S) AND ADDRESS(ES) AFRL/DELS 3550 Aberdeen Ave SE Kirtland AFB NM 87117-5776				10. SPONSOR/MONITOR'S ACRONYM(S)	
				11. SPONSOR/MONITOR'S REPORT NUMBER(S) AFRL-DE-TR-2001-1039	
12. DISTRIBUTION / AVAILABILITY STATEMENT Approved for public release; distribution is unlimited.					
13. SUPPLEMENTARY NOTES					
14. ABSTRACT We demonstrated and delivered high-power (>10W) linear arrays of laser diodes that emit near 1.9 μ m. Significant applications include illuminators for night vision cameras and new sources for gas sensing of such species as HBr, HC1 and H ₂ O. In Phase I we achieved 0.5 W of 300K CW optical power at 1.95 μ m with our "broadened waveguide (BW)" structure. In Phase II we optimized modifications to our Phase I structure and have produced record power outputs in the 0.8 μ m to 1.55 μ m spectrum. This novel structure allows the optical mode to spread out and decreases internal losses from free-carrier absorption. Waveguide parameters were adjusted to permit higher power output at lower threshold and reduced temperature sensitivity. The two-step waveguide active region has lower energy barrier near the quantum wells, which employs "strain-compensated" active regions. Gas source molecular beam epitaxy was to be used to make 1x5 linear arrays of lasers with 200 μ m apertures. Packaging innovations allow extended reliable high-power operation with standard user-friendly commercial semiconductor laser packages.					
15. SUBJECT TERMS Near-infrared, laser diode, broadened waveguide, laser arrays					
16. SECURITY CLASSIFICATION OF:			17. LIMITATION OF ABSTRACT Unlimited	18. NUMBER OF PAGES 24	19a. NAME OF RESPONSIBLE PERSON Andrew Ongstad
a. REPORT Unclassified	b. ABSTRACT Unclassified	c. THIS PAGE Unclassified			19b. TELEPHONE NUMBER (include area code) (505) 853-3207

Table of Contents

1. Program Goals and Technical Objectives	1
2. Phase II Work Plan	1
3. Summary of Phase II Accomplishments	2
4. Results of Phase II.....	4
4.1 Growth of InGaAs/InGaAsP/InP Broadened Waveguide Lasers.....	4
4.1.1 Structure.....	4
4.1.2 Growth of 1.9 μm Laser Structure.....	5
4.2 Laser Fabrication	5
4.3 Laser Characteristics.....	6
4.4 Modified Laser Structure.....	6
4.4.1 Structure.....	6
4.4.2 Device Characteristics	7
4.4.3 CW and Pulsed Results on Single Chip	11
4.4.4 CW and Pulsed Results for a 1x10 Laser Diode Array	12
4.4.5 Pulsed Results for 10x10 Array of 1.9 μm Laser Diodes	13
5. High Power CW 1.9 μm Diode Lasers Commercialization and Business Plan.....	15
5.1 Current Sensors Unlimited Laser Product Lines	15
5.2 Applications of This Program.....	16
5.3 Market Analysis.....	16
5.4 Marketing and Sales Efforts	16
5.5 Capitalization.....	16
6. Conclusions.....	17

List of Figures

Figure 1: Gantt Chart for the Phase II Work Plan of the program.....	1
Figure 2: Internal loss as function of wave guide thickness showing a minimum loss of 2.9 cm^{-1} for a wave guide thickness of 1.2 μm	2
Figure 3: Spectrum of 100 μm stripe laser at 25°C	3
Figure 4: CW and QCW optical power as function of drive current for a 1x10 linear array of 1.9 μm laser diodes	3
Figure 5: QCW optical power as function drive current of a 10x10 stack of 1.9 μm laser diodes before lensing at 22°C and after lensing at 15°C	3
Figure 6: Schematic of the energy bandgap of a two-step active region being developed for high power 1.9 μm lasers	4
Figure 7: Photoluminescence spectra for the two QW probe structure measured at 77 K and 300 K.....	5
Figure 8: Threshold current density for W = 0.9 μm BW 1.9 μm wavelength laser	6
Figure 9: Modified 3 step GRINSCH structure	6
Figure 10: Threshold current density as function of inverse cavity length.....	7
Figure 11: Spectrum from a 100 μm stripe, CW diode Laser at 25°C and 1.4 A.....	7
Figure 12: Internal loss as function of waveguide thickness	8

Figure 13: Internal loss measurements for the broadened waveguide lasers grown under this program.....	9
Figure 14: Temperature dependence of threshold current for a L=1.5mm at $\lambda = 1.95 \mu\text{m}$..	10
Figure 15: Temperature dependence of external quantum efficiency for a L=1.5mm and $\lambda = 1.95 \mu\text{m}$ BW laser.....	10
Figure 16: Optical power versus current curves for 1.9 μm High Power Lasers produced under Phase I of the program. The results are quasi-cw at a temperature of 10°C	11
Figure 17: CW-power and power conversion efficiency of the 100 μm aperture 1.5 mm cavity length laser chip at room temperature.....	11
Figure 18: Pulsed -power and power conversion efficiency of the 100 μm aperture 1.5 cavity length laser chip at room temperature for a duty cycle of 1%.....	12
Figure 19: Pulsed and CW power curves at 25°C and 15°C for a 10 element 1.9 μm diode array	12
Figure 20: The intensity profiles of the 10 element linear array of 1.9 mm laser diodes captured with Sensors Unlimited 2.0 mm cut-off IR-camera.....	13
Figure 21: Peak Power of 10x10 array of 1.95 μm laser diodes at 20°C with 250 μs pulses as function of current and duty cycle.....	13
Figure 22: Picture of 10x10 1.95 μm array of laser diodes taken with a 2 μm cut off IR camera.....	14
Figure 23: Picture of the 10x10 array of 1.9 μm Laser diodes with 10x75 mm focal plane cylindrical lenses in position	14
Figure 24: Peak power output as function of drive current for 10% duty cycle for the unlensed array at 22°C and the lensed array at 15°C	15

1. Program Goals and Technical Objectives

We demonstrated and delivered two high-power (>10W QCW) 1x10 linear arrays and one 100 W (QCW) 10x10 array of laser diodes that emit near 1.9 μm . Significant applications include illuminators for night vision cameras and new sources for gas sensing of such species as HBr, HCl and H₂O. In Phase I we achieved 0.5 W of 300K CW optical power at 1.95 μm with our "broadened waveguide (BW)" structure. In Phase II we optimized modifications to our Phase I structure that has already produced record power outputs in the 0.8 μm to 1.55 μm spectrum. This novel structure allows the optical mode to spread out and decreases internal losses from free-carrier absorption. Waveguide parameters were adjusted to permit higher power output at lower threshold and reduced temperature sensitivity. The two-step waveguide active region has lower energy barrier near the quantum wells, which employs "strain-compensated" active regions. Packaging innovations allow extended reliable high-power operation with standard user-friendly commercial semiconductor laser packages.

2. Phase II Work Plan

Sensors Unlimited and our subcontractor, Princeton University, were to develop a high-power linear laser diode array capable of producing 10 W of optical output with a 25% duty cycle at a wavelength of 1.9 μm . The Phase II work plan is shown in Figure 1. We used a broadened waveguide (BW) approach combined with a step-wise graded index separate confinement heterostructure (GRINSCH). The active region consists of strain-compensated InGaAs/InGaAsP quantum wells. This unique design has reduced internal optical losses because of the broadened waveguide structure, and exhibits increased differential quantum efficiency and lower temperature sensitivity by virtue of the step-wise GRINSCH structure demonstrated successfully in Phase I of the program.

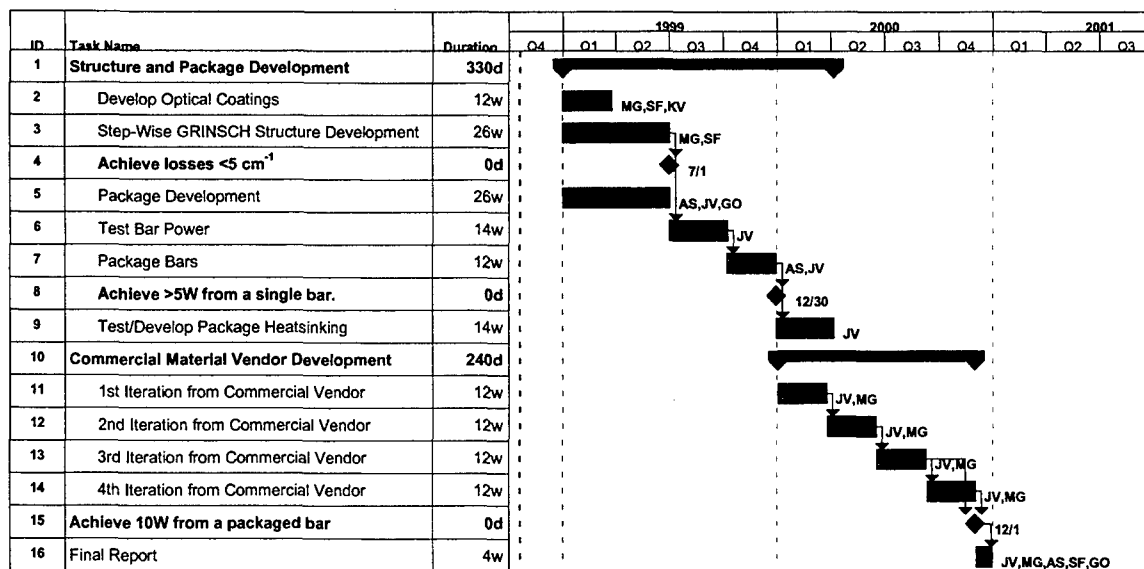


Figure 1. Gantt Chart for the Phase II Work Plan of the program.

As shown above, JV represents the principal investigator, Dr. J. S. Vermaak, AS represents Dr. Alan Sugg, GO represents Dr. Gregory Olsen. SF and MG are Drs. Steve Forrest and Milind Gokhale, respectively, both of Princeton University.

The goal of the first year of the program is to optimize the BW, step-wise GRINSCH laser structure demonstrated in Phase I of the program. The specific milestones for the first year are:

- End of Q2: Achieve internal optical losses of $<5 \text{ cm}^{-1}$.
- End of Year 1: Achieve 5 W from a single 1 cm-wide bar.

During the second year of the program Sensors will began to qualify a commercial vendor for the material system. This effort is a time-consuming and crucial to the ultimate commercial success of the program. The milestones in the second year are:

- End of Q1: Process first iteration of commercial epitaxial material.
- End of Year 2: Demonstrate 10 W from a single 1 cm-wide bar at a 25% duty cycle.

The deliverables under the program include a 1 cm-wide high-power laser array capable of producing 10 W at a 25% duty cycle. In addition, Sensors delivered a package containing 10 bars in a 1 cm x 1 cm array. The emission wavelength of the bars are $1.9 \mu\text{m}$.

3. Summary of Phase II Accomplishments

We have achieved all the goals set out in the Phase II proposal of this project and have delivered two linear arrays of $1.9 \mu\text{m}$ diode lasers emitting $\sim 6\text{W}$ CW and over 11 W QCW optical power. We also delivered a 10×10 array of $1.9 \mu\text{m}$ diode lasers emitting $\sim 100 \text{ W}$ QCW optical power.

The first goal of Phase II was to optimize the BW, step-wise GRINSCH laser structure in order to achieve internal optical losses of $<5 \text{ cm}^{-1}$.

Figure 2 shows that we have achieved this goal by producing a laser structure with internal loss of 2.9 cm^{-1} using a wave guide thickness of $1.2 \mu\text{m}$.

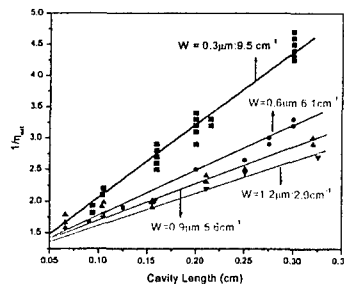


Figure 2. Internal loss as function of wave guide thickness showing a minimum loss of 2.9 cm^{-1} for a wave guide thickness of $1.2 \mu\text{m}$.

Figures 3 and 4 show that we have achieved the second goal of producing a 1 cm-wide high-power linear array of 10x laser diodes operating at $1.9\ \mu\text{m}$ and producing over 10 W of QCW optical power.

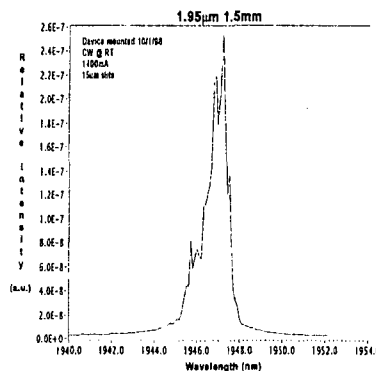


Figure 3. Spectrum of $100\ \mu\text{m}$ stripe laser at 25°C .

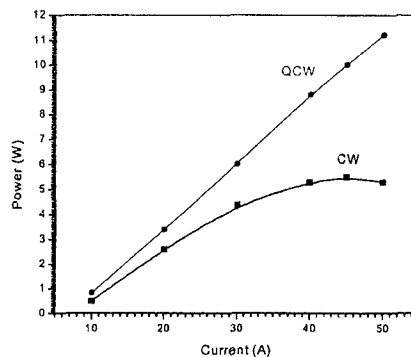


Figure 4. CW and QCW optical power as function of drive current for a 1×10 linear array of $1.9\ \mu\text{m}$ laser diodes.

Figure 5 shows that we have also achieved our third goal of producing a stack of 10×10 high-power linear arrays at the conclusion of the program mounted in a liquid-cooled package of approximate dimensions $1\ \text{cm} \times 1\ \text{cm}$ that deliver 100 W of QCW optical power.

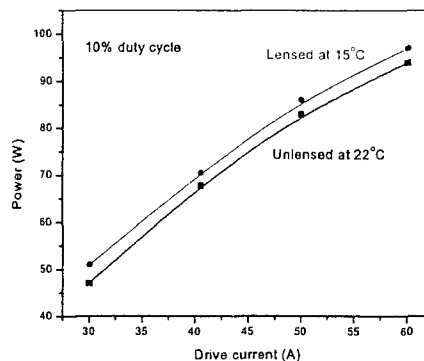


Figure 5. QCW optical power as function drive current of a 10×10 stack of $1.9\ \mu\text{m}$ laser diodes before lensing at 22°C and after lensing at 15°C .

4. Results of Phase II

4.1 Growth of InGaAs/InGaAsP/InP Broadened Waveguide Lasers

4.1.1 Structure

The growth of the InGaAs/InGaAsP/InP BW lasers was done by using a Riber gas-source molecular beam epitaxy (GSMBE) reactor which is equipped with an AsH₃ and PH₃ gas cracker. The reactor is currently also configured with K-cells containing In (2 cells), Ga, Al, Be, and Si. We have successfully grown quantum wells emitting near 1.9 μm . Figure 6 shows the designed active region for the high power laser structure. It consists of a two-step undoped separate confinement heterostructure (SCH) or waveguide sandwiched between highly doped InP cladding regions. The QWs are composed of compressively strained In_{0.75}Ga_{0.25}As layers surrounded by slightly tensile InGaAsP ($\lambda_g = 1.35 \mu\text{m}$) barrier layers. The smaller bandgap of the inner waveguide layer is designed to enable emission longer than 1.9 μm and also provide a graded index profile approximating a GRINSCH (graded index SCH) type active region.

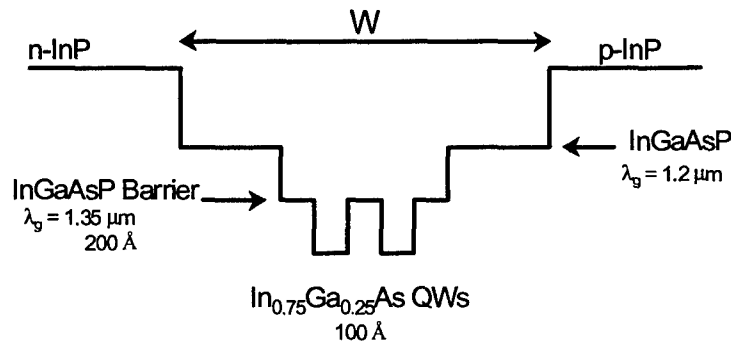


Figure 6. Schematic of the energy bandgap of a two-step active region being developed for high power 1.9 μm lasers.

Since the start of this program, we have developed the growth conditions for the different layers that make up the laser structure shown in Figure 6. Also, a QW probe structure was grown to determine the exact QW thickness for 1.9 μm emission wavelength. In this structure two QWs with different growth times (15 s and 20 s) surrounded by slightly tensile (-0.3%) barrier with bandgap corresponding to 1.35 μm were grown. Figure 7 shows the measured photoluminescence intensity for the two QW structures at 77 K and room temperature. At room temperature both wells emit in the 1.9 μm emission band. The two emission peaks are resolved only at 77 K and the emission energy shows a standard 60-70 meV blue-shift from the 1.9 μm range seen at room temperature.

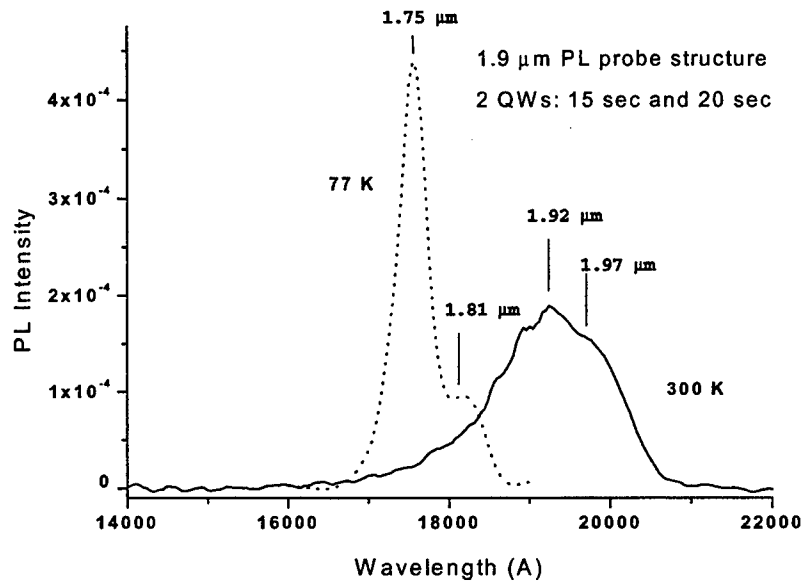


Figure 7. Photoluminescence spectra for the two QW probe structure measured at 77 K and 300 K.

4.1.2. Growth of 1.9 μm Laser Structure

Having obtained the 1.9 μm band emission we grew the laser structure shown in Figure 6. Broadened waveguide lasers with different waveguide widths (W) have been grown to achieve lowest internal loss and highest external quantum efficiency.

The lasers were grown on full 2" epi-ready (100) InP wafers S doped to $n = 5 \times 10^{18} \text{ cm}^{-3}$. The samples were mounted in Indium-free sample holder. After loading, the samples were degassed under vacuum at 250°C for 1 hour, and then introduced into the GSMBE chamber. The oxide was desorbed at $\sim 510^\circ\text{C}$ for 5 min. under 2.6 sccm PH_3 flow. The substrate was then cooled under P_2 flux to 490°C before starting the growth.

4.2. Laser Fabrication

Broad area lasers were fabricated as follows: First, the 100 μm wide stripes were photolithographically defined, and the top p-InGaAsP contact layer between adjacent stripes was removed by etching in $1 \text{ H}_2\text{SO}_4 : 8 \text{ H}_2\text{O}_2 : 40 \text{ H}_2\text{O}$ (etch rate: $0.4 \mu\text{m}/\text{min}$). Next, a 3000 \AA thick SiN_x mask was deposited using plasma enhanced chemical vapor deposition, followed by etching 100 μm -wide stripes to expose the p^+ -InGaAsP. The p-type metal contact to the stripes was a non-alloyed contact using 200 \AA Ti: 500 \AA Ni : 2000 \AA Au deposited by e-beam evaporation. The wafer was then thinned to $\sim 100 \mu\text{m}$, and the back contact (270 \AA :Ge / 450 \AA :Au / 215 \AA :Ni / 1000 \AA :Au) was deposited, and the contact metals were annealed at 360°C for 60 seconds. Finally, laser bars were cleaved and characterized.

4.3. Laser Characteristics

The threshold current density as a function of inverse cavity length for uncoated lasers from the BW laser structure, is shown in Figure 8. Due to the reduction in the optical confinement factor for the quantum wells, J_{th} for BW lasers the threshold current density is slightly higher than conventional 1.9 μm lasers. However, it is largely unaffected for long cavity length ($L > 2$ mm) devices, with a value of 300 A/cm^2 achieved for 3.3 mm long laser.

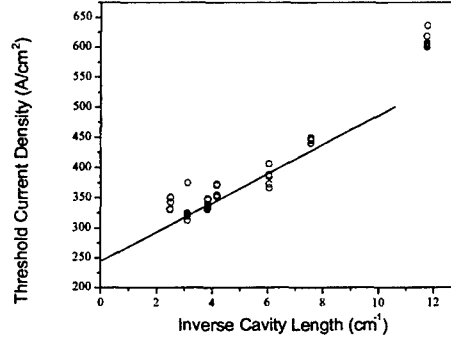


Figure 8. Threshold current density for $W = 0.9$ μm BW 1.9 μm wavelength laser.

4.4. Modified Laser Structure

4.4.1. Structure

In this section we describe a new device structure capable of high power operation. Figure 9 shows the designed active region for this high power laser structure. The waveguide or separate confinement heterostructure (SCH) layer region is comprised of a higher bandgap waveguide layers to reduce internal loss from free carrier absorption in the waveguide layer and improve the temperature sensitivity of threshold current and external efficiency. We started by growing a series of thick InGaAsP layers to achieve a lattice-matched quaternary with a bandgap corresponding to 1.05 μm or 1.18 eV. For the barrier layer, we retained the InGaAsP ($\lambda_g = 1.35$ μm) quaternary found in the first structure. We then grew a 1.95 μm wavelength broadened waveguide laser structure.

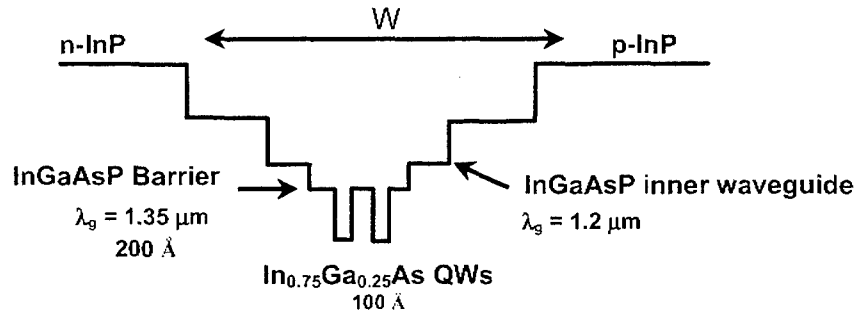


Figure 9. Modified 3 step GRINSCH structure.

The laser structure consist of a separate confinement waveguide layer of thickness W ($0.9\text{ }\mu\text{m}$), and lattice-matched InGaAsP composition corresponding to $\lambda_g = 1.05\text{ }\mu\text{m}$. The active region is bound by $1.5\text{ }\mu\text{m}$ thick InP cladding layers. The active region is comprised of two, compressively strained, $90\text{ }\text{\AA}$ thick InGaAs wells separated by $200\text{ }\text{\AA}$ thick barriers made of InGaAsP ($\lambda_g = 1.35\text{ }\mu\text{m}$).

In order to investigate the influence of the waveguide thickness (W), on the internal loss, several lasers structures with $W = 0.3\text{ }\mu\text{m}$, $0.6\text{ }\mu\text{m}$, $0.9\text{ }\mu\text{m}$ were grown. After laser fabrication as described in section 4.2 they were fully characterized with the results, described in 4.4.2

4.4.2 Device Characteristics

The threshold current densities versus cavity length for these lasers are plotted in Figure 10.

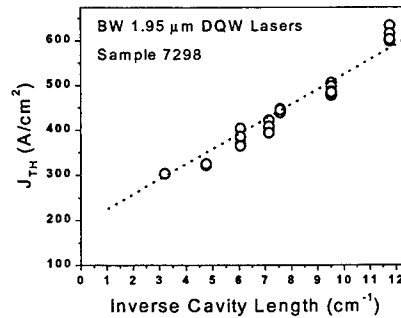


Figure 10. Threshold current density as function of inverse cavity length.

From Figure 10 we can see that the threshold current density for long cavity lasers is of the order of 300 A/cm^2 .

It can be seen in Figure 11 that the lasing wavelength for the lasers is $1.95\text{ }\mu\text{m}$.

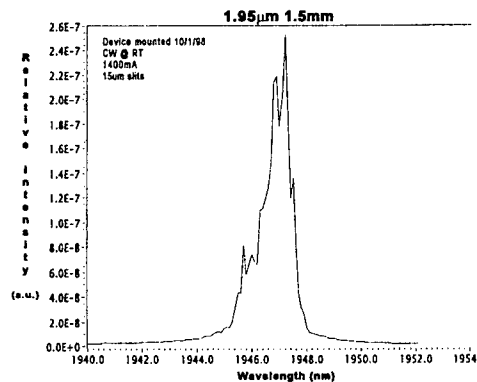


Figure 11. Spectrum from a $100\text{ }\mu\text{m}$ stripe, CW diode Laser at 25°C and 1.4 A .

Figure 12 depicts the internal loss as function of waveguide thickness for these devices.

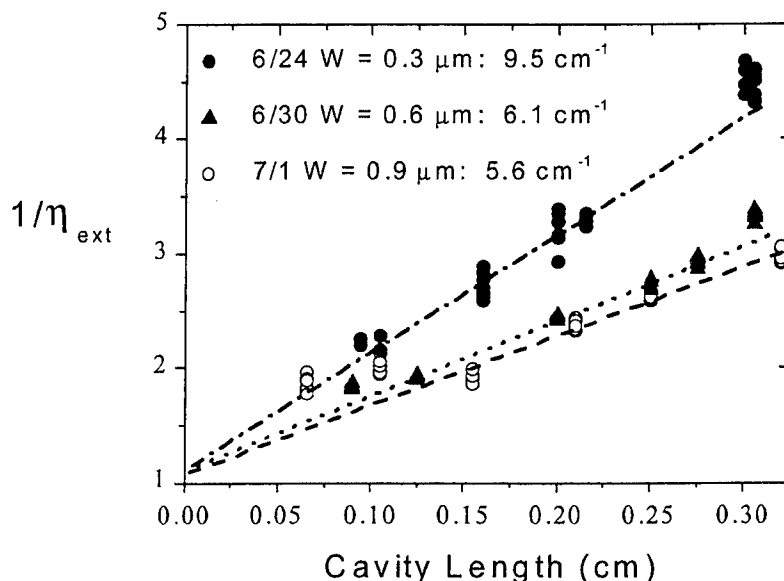


Figure 12. Internal loss as function of waveguide thickness.

The internal efficiency and optical loss were determined from Figure 12. As can be seen from the figure, the internal loss for these lasers dropped from 9.5 cm^{-1} to 5.6 cm^{-1} when the waveguide thickness is increased from 0.3 μm to 0.9 μm . For all lasers the internal efficiency is $\eta_i = 75\text{-}80\%$. The internal loss of the lasers is about 5.6 to 7.5 cm^{-1} for a waveguide width of 0.9 μm . This internal loss is still too high to make a very efficient high power laser. This loss should be further reduced to approximately 2 to 3 cm^{-1} to achieve sufficient output power.

The high output losses seen in these lasers suggested that an internal loss mechanism, other than loss caused by free carrier absorption in the highly doped cladding region, must be present. One possible loss could be *scattering loss* due to index changes in material along the length of the lasers, or surface defects that scatter the laser mode and result in additional loss. However, given that all lasers of a given length measured on a bar had almost the same threshold current and differential efficiency (i.e. very little scatter in experimental data), scattering loss at least caused by random surface defects might not be present. We then decided to carefully examine the spectra to see if any non-uniformity in the thickness of the 2 QWs is present. We found that just after threshold we have a clean output lasing spectra with only one peak. However, at about 1.05 times threshold current a second peak at a shorter wavelength (-3 nm from the first) appears. This suggests that the two QWs we are growing are not of the same thickness but at least one is wider than the others. This QW with the lowest energy state lases first but the other QWs have not reached transparency and act as a drag on the first QW. At 1.3 times threshold current the FWHM of the spectra is 6 nm which is too broad and has to be narrowed for efficient high power laser operation.

We have never seen such a variation in QW thickness in all our previous lasers at 1.3 μm , 1.55 μm , 0.98 μm or 0.89 μm wavelength. The thickness variation between the first well (in the growth sequence) and the subsequent wells is caused by an unacceptably high flux transients from our Ga and In cells. The shutters on these cells moved due to loose set-screws in the shutter assembly and rested right on top of the cell mouth. When the cells first open, the initial flux is much higher (about 10% more) due to heat reflected from the molybdenum shutters back on to the molten charge. When the cell opens the charge radiatively cools down and subsequently the next QWs and barriers are grown at a lower growth rate. This transient had very little effect on our earlier high power 0.98 μm lasers as the shutters were further apart from the mouth of the cells. But the higher transients with shutters so close to sources have caused this new undesirable effect on the QW emission spectra. We validated this hypothesis by growing a BW laser with only one QW. Also, we vented the MBE system to fix the shutter problem and performed other routine maintenance.

Figure 13 shows a dramatic improvement in internal optical losses from lasers that were grown after the routine maintenance on the MBE. The loss has been reduced from 5.2 cm^{-1} to below 3 cm^{-1} and these results confirm the validity of our design approach for the Phase II proposal. The devices were mounted p-down on Cu heat sinks and operated at 10°C.

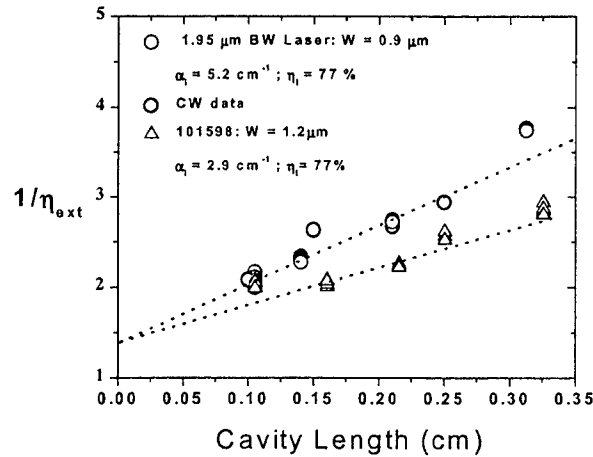


Figure 13. Internal loss measurements for the broadened waveguide lasers grown under this program.

Important performance characteristics of a semiconductor laser such as threshold current density and external quantum efficiency are dependent on operating temperature. The temperature dependence of a laser is empirically defined as $J_{\text{TH}}(T) = J_0 \text{Exp}(T/T_0)$, where T_0 is the characteristic temperature. For high power operation, a semiconductor laser must have a high T_0 and more importantly a weak temperature dependence of external quantum efficiency. Such lasers with high power-conversion efficiency can be operated CW using only a TE cooler. High power operation without a liquid cooled heat sink is highly desirable since these lasers can be made compact, rugged and less expensive.

Figure 14 shows the characteristic temperature of BW ($W = 0.9 \mu\text{m}$) of $1.9 \mu\text{m}$ wavelength high power laser with a cavity length of 1.5 mm . For the temperature range of normal operation (10°C - 35°C) a reasonably high T_0 value of 60 K is obtained. This is slightly greater than the 50 K reported for standard $1.9 \mu\text{m}$ wavelength lasers

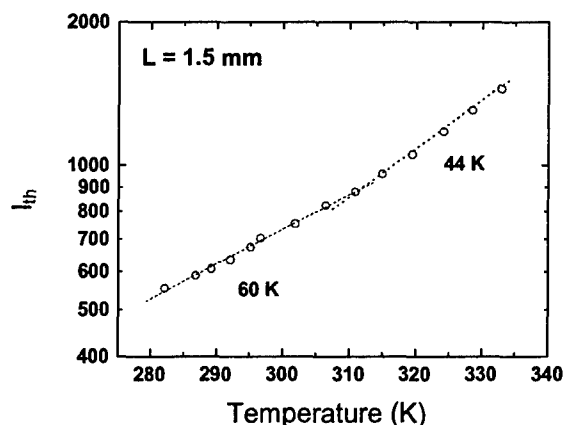


Figure 14. Temperature dependence of threshold current for a $L=1.5\text{mm}$ at $\lambda = 1.95 \mu\text{m}$.

Figure 15 shows the temperature dependence of the external quantum efficiency for a 1.5 mm long laser. The external quantum efficiency is strongly dependent on the operating temperature suggesting that these $1.9 \mu\text{m}$ lasers will yield the highest output power when run on a temperature controlled heat sink kept at 10°C .

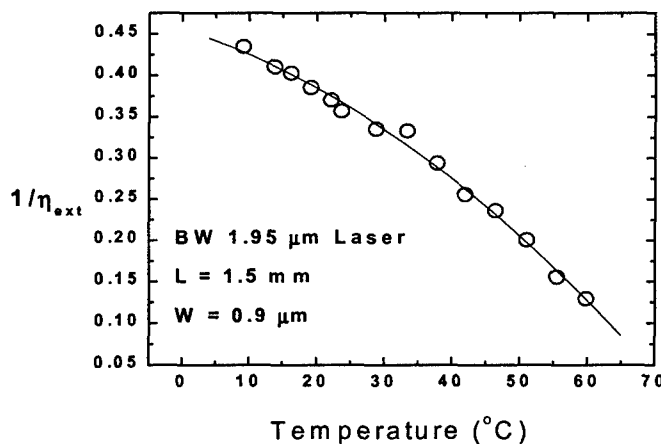


Figure 15. Temperature dependence of external quantum efficiency for a $L=1.5\text{mm}$ and $\lambda = 1.95 \mu\text{m}$ BW laser.

Figure 16 shows a total power level (both facets) of 3 W with a 1% duty cycle from a $100 \mu\text{m}$ aperture with uncoated facets. We measured 2 W with a duty cycle of 25% . The

pulses for the 25% duty cycle are a standard configuration (i.e. the device is on for the initial 25% of the period, and off for the final 75%).

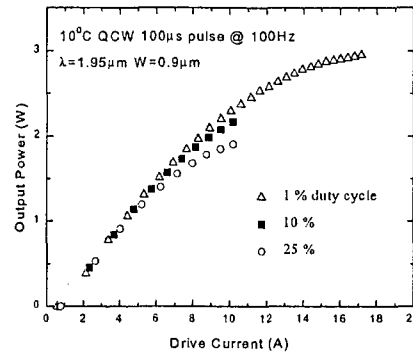


Figure 16. Optical power versus current curves for 1.9 μm High Power Lasers produced under Phase I of the program. The results are quasi-cw at a temperature of 10°C.

After processing we found that the chips had a very high series resistance of $\sim 0.18 \Omega$. This is due to a lower doping used in the p-contact layer. In the next growth cycle we used highly doped (10^{18}) InGaAs as p-contact layer instead of InGaAsP. Using a rapid thermal anneal (RTA) oven, both the p-contact and the n-contact was annealed for 30 s at 425°C and 340°C, respectively. This procedure dropped the series resistance from 0.18Ω to 0.073Ω while the specific resistance of the laser was measured to be $5 \times 10^{-5} \Omega\text{cm}^2$.

4.4.3 CW and Pulsed Results on Single Chip

A wafer with a laser structure as depicted in Figure 9 was grown as described in section 4.1.2 100 μm wide striped lasers with cavity lengths of 1.5 mm were fabricated as described in section 4.2. The chips were mounted p-side down on C-mounts and characterized in CW and pulsed modes.

Figure 17 depicts the CW-power and power conversion efficiency of the 100 μm aperture 1.5 cavity length laser chip at room temperature.

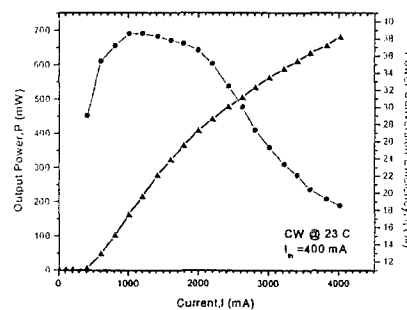


Figure 17. CW-power and power conversion efficiency of the 100 μm aperture 1.5 mm cavity length laser chip at room temperature.

From Figure 17 it can be seen that the threshold current for the laser is 400 mA while the maximum power conversion efficiency is 38% around 1000 mA drive current. Due to heating effects, the efficiency starts to drop drastically for drive currents higher than 2000 mA, which again just emphasizes the fact that good thermal management is essential in obtaining high CW and QCW-powers.

Figure 18 depicts the pulsed -power and power conversion efficiency of the 100 μm aperture 1.5 cavity length laser chip at room temperature for a duty cycle of 1%.

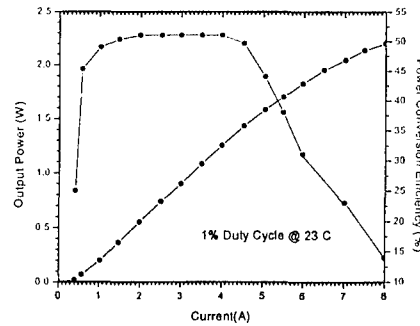


Figure 18. Pulsed -power and power conversion efficiency of the 100 μm aperture 1.5 cavity length laser chip at room temperature for a duty cycle of 1%.

The power efficiency is over 50% for drive currents 1 to 5 A with maximum power of 2.2 W at 8 A

4.4.4 CW and Pulsed Results for 1x10 Laser Diode Array

We have processed 1 cm wide arrays that contain ten individual 100 μm wide stripe contacts with 1 mm center to center separation. The processed wafer was cleaved into bars with cavity length 1.5 mm and the mirror facets were coated with high-reflectivity (HR-95%) and anti-reflective (AR-3%) coatings. Figure 19 shows the CW and pulsed powers of one of the 10 element bars obtained at 25°C and 15°C.

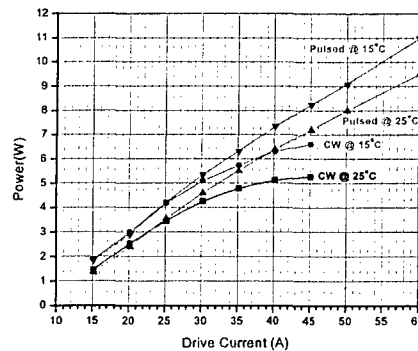


Figure 19. Pulsed and CW power curves at 25°C and 15°C for a 10 element 1.9 μm diode array.

Figure 20 shows the intensity profiles of the 10 element linear array of 1.9 μm laser diodes captured with Sensors Unlimited 2.0 μm cut-off IR-camera.

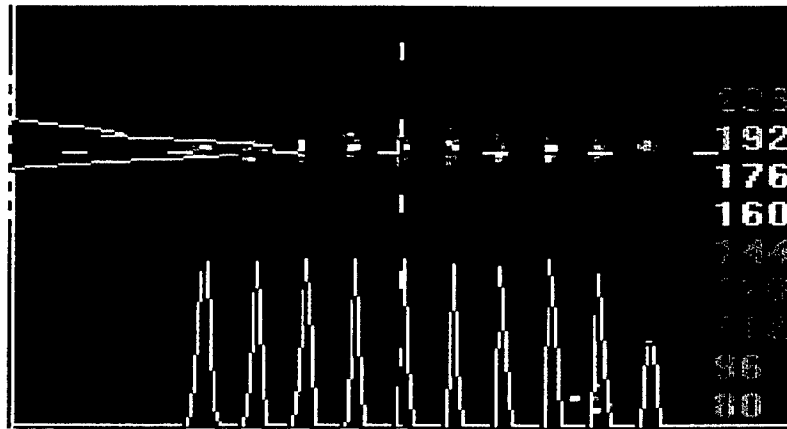


Figure 20. The intensity profiles of the 10 element linear array of 1.9 mm laser diodes captured with Sensors Unlimited 2.0 mm cut-off IR-camera.

4.4.5 Pulsed Results for 10x10 Array of 1.9 mm Laser Diodes

We fabricated a stacked array of ten of these bars to produce a matrix of 10x10 laser diodes.

Figure 21 depicts the peak power as function of pulsed rate and current at 20°C.

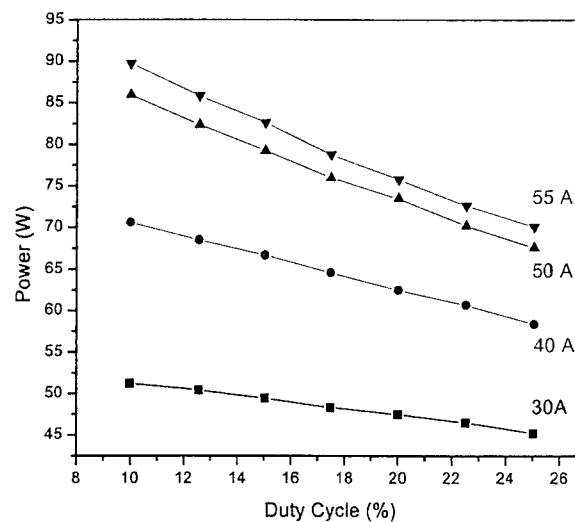


Figure 21. Peak Power of 10x10 array of 1.95 μm laser diodes at 20°C with 250 μs pulses as function of current and duty cycle.

The highest peak power of 90 W was obtained at a duty cycle of 10% and drive current of 55 A. The heating of the array at higher duty cycles causes the power drop of approximately 20%.

The fast axis of all the diodes in the 10x10 array were focused using a cylindrical lens with a 75 mm focal length. Figure 22 is a picture of the 10x10 array taken with our 2 μm cutoff 320x240 pixel NIR camera.

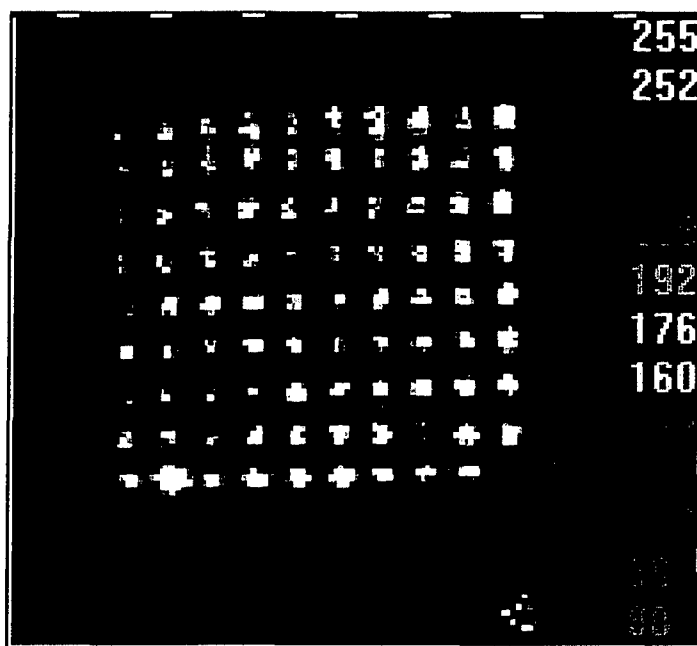


Figure 22. Picture of 10x10 1.95 μm array of laser diodes taken with a 2 μm cutoff NIR camera.

The fast axis of all the diodes in the 10x10 array were focused using a cylindrical lens with a 75 mm focal length. Figure 23 is a picture of the 10x10 array with the cylindrical lenses in position.

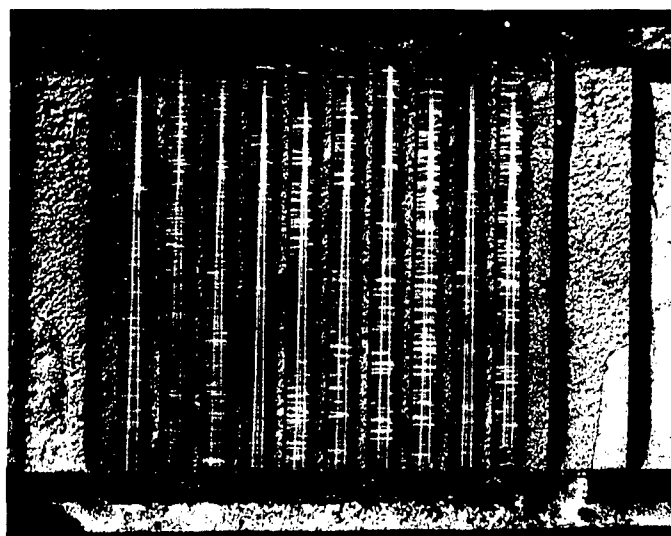


Figure 23. Picture of the 10x10 array of 1.9 μm Laser diodes with 10x75 mm focal plane cylindrical lenses in position.

Figure 24 depicts the peak power output as function of drive current for 10% duty cycle for the unlensed array at 22°C and the lensed array at 15°C. The lensed array give a maximum power output of 97 W at 15°C, which is close to the 100 W we originally set out to achieve.

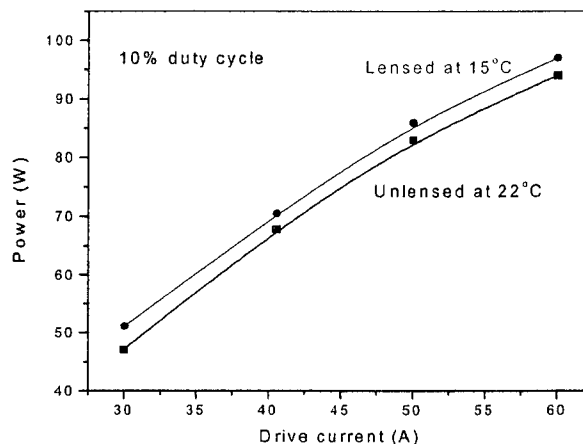


Figure 24. Peak power output as function of drive current for 10% duty cycle for the unlensed array at 22°C and the lensed array at 15°C.

5. High Power CW 1.9 μm Diode Lasers Commercialization and Business Plan

5.1 Current Sensors Unlimited Laser Product Lines

Sensors Unlimited, Inc. is a leading supplier of diode lasers for laser-absorption molecular spectroscopy gas-sensing applications. Gases such as CO, H₂O, CH₄, H₂S, HCl, HF, HBr and NH₃ are currently monitored using near-infrared (NIR) laser-diode based systems in the 0.75 μm – 2.0 μm wavelength range. These systems achieve gas detection levels in the part-per-million (ppm) range by monitoring absorption of the overtone optical transition of these molecules. Several of the important applications for trace-gas sensing are listed below:

- Monitoring of important industrial chemicals such as: CO, H₂O, CH₄, H₂S, HCl, HF, HBr and NH₃.
- Monitoring of some of the more than 400 trace gases on the human breath for medical diagnostics, such as ¹³CO₂ and ¹²CO₂ at 2 μm .
- Detecting explosives in which the catalytically decomposed constituents of the explosives, RDX for example, are detected. These constituents are NO, N₂O, NO₂, and HCN, which all have absorption lines in the 1.8 μm to 2.1 μm near-infrared wavelength range. These applications require single-mode outputs of about 5 mW.

5.2. Applications of This Program

The lasers produced under this program will be ideal for use as eye-safe illuminators with the 2.0 μm camera being developed at Sensors Unlimited for industrial and military surveillance applications.

5.3 Market Analysis

Sensors Unlimited, Inc. has a strong history in the laser diode business. Since 1992, we have had a strategic relationship with Sarnoff Corporation to provide DFB and Fabry-Perot lasers specifically targeted at the laser absorption spectroscopy trace-gas sensing markets. In 1997, Sensors had revenue from lasers of nearly \$600,000. The revenue from laser sales in 1998 dropped by nearly 50%, in large part due to the decision to discontinue delivery of fiber-coupled lasers. Fiber-coupled lasers constituted nearly 80% of product sales in lasers in 1997. The decision to discontinue deliveries of fiber-coupled lasers was due to the difficulties of delivering reliably fiber-coupled laser packages. We are in the process of developing a silicon v-groove fiber assembly that will allow Sensors to offer a fiber-coupled product line. We anticipate the introduction of this fiber-coupling technology to the product line by the end of 2000. This will position Sensors for solid laser diode revenue growth for 2001 and beyond.

5.4 Marketing and Sales Efforts

Sensors Unlimited, Inc has the necessary expertise to market products resulting from this program. We presently have a database of over 6000 potential (and actual) customers. This has been compiled from a three-year marketing effort that included color advertisements in trade journals such as *Laser Focus*, *Photonics Spectra* and *Spectroscopy*, trade shows such as SPIE (Orlando and San Diego), and the *IEEE* Boston OPTCON/LEOS meeting, CLEO and numerous "New Product" announcements in trade journals such as *Fiber Optic Product News* and *Semiconductor International*. We have a distribution list of over 50 trade journals that get copies of any of our new product announcements.

This product line serves a technology intensive market segment. Sensors employs experts in the field of semiconductor lasers and the attendant photodiode technology necessary to address these markets. Pro-active sales is used to identify and target potential clients by comparing their existing technology to the laser based gas sensing technology.

5.5 Capitalization

Sensors Unlimited has sold commercial products since 1992. Our *product* sales are growing nearly 50% per year (\$24 million in 2000) and are based *entirely* on products generated from SBIR support. We have been successful with this system because we only pursue topics that are ultimately in our business interests - covering infrared sensing and intelligent information processing. In October, 2000 Sensors Unlimited was acquired by Finisar Corp.

6. Conclusions

We were able to optimize the BW, step-wise GRINSCH laser structure in order to achieve internal optical loss of 2.9 cm^{-1} using a wave guide thickness of $1.2 \text{ }\mu\text{m}$. From this material we produced a 1 cm-wide high-power linear array of 10x laser diodes operating at $1.9 \text{ }\mu\text{m}$ and producing over 10 W of QCW optical power.

We also produced a stack of 10x10 high-power linear arrays at the conclusion of the program, mounted in a liquid-cooled package of approximate dimensions 1 cm x 1 cm that deliver 100 W of QCW optical power.

We can thus conclude that we have achieved all the goals set out in the Phase II proposal of this project and have delivered two linear arrays of $1.9 \text{ }\mu\text{m}$ diode lasers emitting $\sim 6 \text{ W}$ CW and over 11 W QCW optical power and a 10x10 array of $1.9 \text{ }\mu\text{m}$ diode lasers emitting $\sim 100 \text{ W}$ QCW optical power.

DISTRIBUTION LIST

DTIC/OCF

8725 John J. Kingman Rd, Suite 0944

Ft Belvoir, VA 22060-6218

1 cy

AFSAA/SAMI

1570 Air Force Pentagon

Washington, DC 20330-1580

1 cy

AFRL/VSIL

Kirtland AFB, NM 87117-5776

2 cys

AFRL/VSIIH

Kirtland AFB, NM 87117-5776

1 cy

Sensors Unlimited, Inc.

Attn: Ms. Joanne Bender

3490 U.S. Route 1, Building 12

Princeton, NJ 08540

1 cy

Official Record Copy

AFRL/DELS

3 cys